Journal of Medicinal Chemistry

Article

Asymmetric Hydroboration Approach to the Scalable Synthesis of ((1*R*, 3*S*)-1-Amino-3-((*R*)-6-hexyl-5, 6, 7, 8-tetrahydronaphthalen-2-yl)cyclopentyl)methanol (BMS-986104) as a Potent S1P Receptor Modulator

Michael G. Yang, Zili Xiao, T. G. Murali Dhar, Hai-Yun Xiao, John L Gilmore, David Marcoux, Jenny H. Xie, Kim W. McIntyre, Tracy L. Taylor, Virna Borowski, Elizabeth Heimrich, Yu-Wen Li, Jianlin Feng, Alda Fernandes, Zheng Yang, Praveen V. Balimane, Anthony M. Marino, Georgia Cornelius, Bethanne M. Warrack, Arvind Mathur, Dauh-Rurng Wu, Peng Li, Anuradha Gupta, Bala Pragalathan, Ding Ren Shen, Mary Ellen Cvijic, Lois D. Lehman-McKeeman, Luisa M. Salter-Cid, Joel C. Barrish, Percy H Carter, and Alaric J. Dyckman

Just Accepted

1
2
3
4
5
6
7
8
9
10
11
12
13
14
15
16
17
18
19
20
21
22
23
24
25
26
27
28
29
30
31
32
33
34
35
36
37
38
39
40
41
42
43
44
45
46
47
48
49
50
51
52
53
54
55
56
57
58
59
60

Development, Leads Discovery & Optimization
Lehman-McKeeman, Lois; Bristol-Myers Squibb Company, Investigative Toxicology (MS H24-03)
Salter-Cid, Luisa; Bristol-Myers Squibb Pharmaceutical Research and Development, Discovery Biology
Barrish, Joel; Achillion Pharmaceuticals Inc
Carter, Percy; Bristol-Myers Squibb Company
Dyckman, Alaric; Bristol-Myers Squibb, Discovery Chemistry

SCHOLARONE™
Manuscripts

Asymmetric Hydroboration Approach to the Scalable Synthesis of ((1*R*, 3*S*)-1-Amino-3-((*R*)-6-hexyl-5, 6, 7, 8-tetrahydronaphthalen-2-yl)cyclopentyl)methanol (BMS-986104) as a Potent S1P₁ Receptor Modulator

Michael G. Yang,* Zili Xiao, T. G. Murali Dhar, Hai-Yun Xiao, John L. Gilmore, David Marcoux, Jenny

H. Xie, Kim W. McIntyre, Tracy L. Taylor, Virna Borowski, Elizabeth Heimrich, Yu-Wen Li, Jianlin Feng,

Alda Fernandes, Zheng Yang, Praveen Balimane, Anthony M. Marino, Georgia Cornelius, Bethanne M.

Warrack, Arvind Mathur, Dauh-Rurng Wu, Peng Li, Anuradha Gupta, Bala Pragalathan, Ding Ren Shen,

Mary Ellen Cvijic, Lois D. Lehman-McKeeman, Luisa Salter-Cid, Joel C. Barrish, Percy H. Carter, and

Alaric J. Dyckman*

Research and Development, Bristol-Myers Squibb Company, Princeton, New Jersey 08543-4000, United States

ABSTRACT: We describe a highly efficient route for the synthesis of **4a** (BMS-986104). A key step in

the synthesis is the asymmetric hydroboration of trisubstituted alkene **6**. Particularly given the known

difficulties involved in this type of transformation (**6 → 7**), the current methodology provides an efficient

approach to prepare this class of compounds. In addition, we disclose the efficacy of **4a** in a mouse EAE

model, which is comparable to **4c** (FTY720). Mechanistically, **4a** exhibited excellent remyelinating effects

on lysophosphatidylcholine (LPC)-induced demyelination in a three-dimensional brain cell culture assay.

INTRODUCTION

Multiple sclerosis (MS) is a chronic, debilitating disease of the central nervous system (CNS), which

affects more than two million people worldwide.[1] Studies have shown that B and T cells play a significant

role in MS pathogenesis and T cells are significantly elevated during disease development.[2,3] Upon

entering the CNS, T cells are reactivated by activated antigen-presenting cells resulting in overproduction

of cytokines and initiation of inflammatory processes.[4,5] Sphingosine-1-phosphate (S1P) is known to

transduce extracellular signals through its interactions with five related G-protein-coupled receptors (S1P₁₋

₅).[6] Studies have shown that the S1P₁ receptor is essential for regulating T cell egress from secondary

lymphoid organs.[7] FTY720 (**4c**) is a once-daily oral drug for the treatment of MS.[8] The phosphate form of FTY720 (**4c**-P) is a full agonist of $S1P_1$, showing maximal response in in vitro assays compared to the endogenous ligand S1P, and it induces complete $S1P_1$ receptor internalization.[9] Unlike S1P, agonism with **4c**-P (FTY720-P) induces prolonged desensitization without recycling, thus acting as powerful functional antagonist to block $S1P/S1P_1$ signaling. As a result of this functional antagonism, **4c** (FTY720) inhibits T cell egress from thymus and lymph nodes, thereby reducing T cell infiltration into the CNS.[10] Compound **4c** is also known to promote remyelination by acting directly on the cells of the central nervous system, an effect that is believed to contribute to clinical efficacy of **4c** in MS.[11] Therapeutic efficacy of **4c** has also been demonstrated in various animal models of disease, such as rheumatoid arthritis, inflammatory bowel disease, lupus, and atherosclerosis.[12-14] Clinical studies have demonstrated an adverse pulmonary and cardiovascular safety profile of **4c** that includes decrease of pulmonary function, transient bradycardia and sustained elevation of blood pressure.[15] With the objectives of eliminating or reducing the unwanted side-effects, we recently described the synthesis of tetrahydronaphthalene-based amino-cyclopentylmethanol **4a** (BMS-986104) and its associated research findings as a potent, differentiated, modulator of $S1P_{1,4,5}$ (Figure 1).[16,17] In vitro, the phosphorylated metabolite of **4a**, formed through the action of sphingosine kinase 2,[18] displayed ligand-biased signaling at $S1P_1$, including partial agonism in GTPγS and receptor internalization assays, as well as a reduced predicted liability for heart rate effects based on a human-relevant cardiomyocyte assay. In vivo, pulmonary edema in rodent that was noted after oral administration with full agonists of $S1P_1$ (including **4c**) was absent with **4a**.

**Figure 1.** Original synthetic route for the synthesis of **4a**.
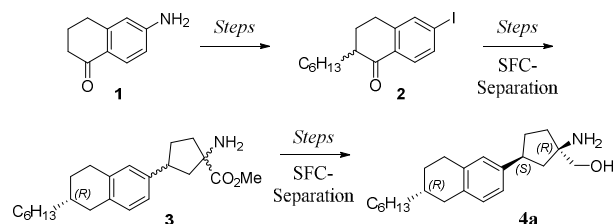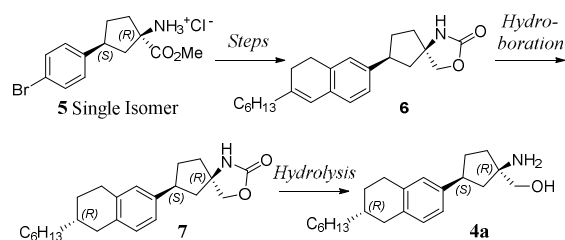
Figure 2. Improved synthetic route for the synthesis of **4a**.

In our previous communication, we reported the in vivo efficacy of **4a** in a rodent model of colitis and the synthetic route used for the preparation of **4a** (Figure 1).[17] The described synthesis of **4a** was non-stereoselective and the overall yield was low (<1% yield in 11-steps). Furthermore, we had to rely on multiple chiral separations to obtain the isomerically pure product (**4a**). Since the therapeutic efficacy of **4a** was only studied in a T cell transfer colitis model at that time, we were also interested in expanding our research to include additional animal models of disease, namely the mouse experimental autoimmune encephalomyelitis (EAE) model for MS. An improved synthesis of **4a** to provide material in support of these studies was desired. In this publication, we describe an efficient synthesis of **4a** and highlight the methodology development of an asymmetric hydroboration of tri-substituted alkene **6** (Figure 2, **6** → **7**). The current investigation also describes the in vitro findings of **4a** and its in vivo results associated with the EAE model.

Scheme 1. Synthesis of β-tetralone **14**.
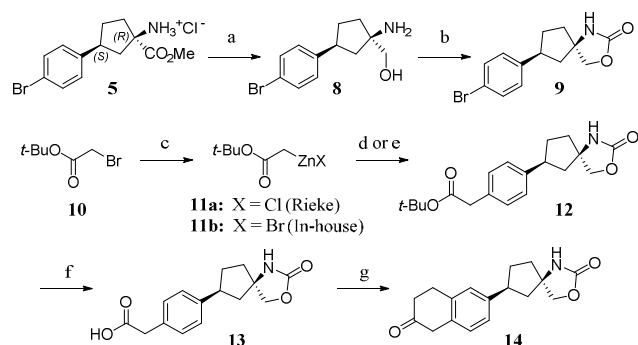
Reagents and conditions: a) step-1: K_2CO_3, H_2O; step-2: $NaBH_4$, MeOH, 87% yield for two steps. b) CDI, Dioxane, 97% yield. c) Zn, TMSCl, THF, 80 °C, 1h, 63% yield. d) LiHMDS, THF, **9** and **11a** followed by $Pd_2(dba)_3$, Q-phos, Dioxane, 80 °C, 10-85% yield. e) LiHMDS, THF, **9** and **11b** followed by $Pd_2(dba)_3$, Q-phos, Dioxane, 80 °C, 94-100% yield. f) TFA, CH_2Cl_2, 96% yield. g) step-1: oxalyl chloride; step-2: ethylene, $AlCl_3$, CH_2Cl_2, -78 °C to rt, 64% yield for two steps.

CHEMISTRY

The revised synthetic approach for the preparation of **4a** started with the synthesis of intermediate **14** (Scheme 1). Compound **5** was prepared using the procedures described in the literature.[19] Treatment of amino methyl ester HCl salt **5** with aqueous K_2CO_3 and then sodium borohydride provided primary alcohol **8** in 87% yield. CDI-promoted cyclization gave **9** in 97% yield. Reformatsky reaction with arylbromide **9** and *tert*-butyl chlorozincacetate (**11a**) completed the initial synthesis of **12**. The organozinc chloride solution of **11a** is commercially available, but is costly ($780 $\rightarrow$ 50 mL, 0.5 M solution). In our experience, **11a** was only stable at low temperature and for relatively short duration. As a result, the reaction yields of the Reformatsky reaction ranged from 10–85%, depending upon the quality of **11a**. In order to reduce the cost and control the quality of the organozinc reagent, we explored other alternatives for the preparation of a comparable organozinc reagent. Using a slightly modified procedure from the literature,[20] we were able to make more than 150 grams of *tert*-butyl bromozincacetate (**11b**) from commercially available α-bromo ester **10**. The synthesis of **11b** was typically carried out using 15 grams of α-bromo ester **10** for each trial. As a solid, *tert*-butyl bromozincacetate **11b** was easy to handle, inexpensive to make, and stable at room temperature for weeks. More importantly, the coupling reaction of **9** (10 g, 33.8 mmol) with **11b** proceeded smoothly to give the desired product **12** in 94–100% yield, consistently in multiple trials. Deprotection of **12** with TFA gave acid **13**. Reaction of **13** with oxalyl chloride provided the corresponding acid chloride, which was treated with ethylene and $AlCl_3$ to provide β-tetralone **14** in 64% yield for the last two steps.

Scheme 2. Asymmetric hydroboration approach to compound **4a**.
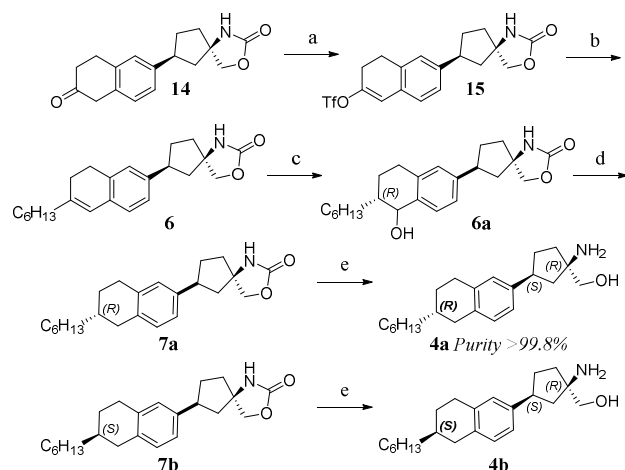
Reagents and conditions: a) LDA, DMPU, -78 °C followed by PhN(Tf)$_2$, -78 → 0 °C, 69% yield. b) LiHMDS, Fe(acac)$_3$, THF/NMP, C$_6$H$_{13}$MgBr, -40 °C, 94% yield. c) S-Ipc-BH$_2$, BF$_3$·OEt$_2$, -40 °C, CH$_2$Cl$_2$ followed by H$_2$O$_2$, NaOH, rt, 30 min, 87% yield. d) step-1: H$_2$/Pd-C, rt, MeOH; Step-2: Chiral OJ-H (5 μm), CO$_2$/[IPA:ACN 1:1 w 0.1% TFA] (90:10), 35 °C, 100 bars, PK1. 77% for two steps. e) NaOH, Dioxane, 95% yield.

Table 1. Asymmetric Hydrogenation or Hydroboration of **6**
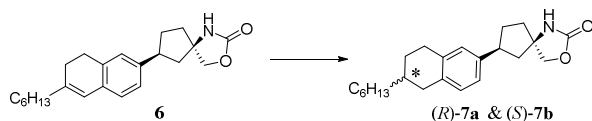
Entry	Reducing Agents	Reaction Conditions^a	(R) : (S) ratio
1	H$_2$, Pd(OH)$_2$	MeOH, rt, 1 h	1 : 1
2	H$_2$, catASium® MNXyIF(R)-Rh	MeOH, rt, 900 psi, 16 h	2 : 1
3	Catecholborane^b (S)-BINAP	THF, rt → 80 °C, 16 h → Step 2 & Step 3	no product
4	(S)-Alpine-Boramine	CH$_2$Cl$_2$, rt → 55 °C, 16 h → Step 2 & Step 3	no product
5	(S)-Ipc-BH$_2$	CH$_2$Cl$_2$, rt, 0 °C, 2 h → Step 2 & Step 3	3 : 1
6	(S)-Ipc-BH$_2$	CH$_2$Cl$_2$, -30 °C, 6 h → Step 2 & Step 3	8 : 1
7	(S)-Ipc-BH$_2$	THF, -30 °C, 6 h → Step 2 & Step 3	no product

^{a}Step-2: H$_2$O$_2$, NaOH, rt, 30 min. Step-3: H$_2$/Pd-C, H$_2$, rt, MeOH. ^{b}Bis(1,5-cyclooctadiene)rhodium(I) tetrafluoroborate.

The asymmetric synthesis of compound **4a** from **14** is outlined in Scheme 2.   The LDA-promoted triflation reaction of **14** with phenyl triflimide gave **15** in 69% yield. Intermediate **15** was then treated with LiHMDS followed by Fe-catalyzed coupling with hexylmagnesium bromide to give **6** in 94% yield, which was used for the next reaction without further purification.   With intermediate **6** in hand we were in a position to explore chiral reagent-based asymmetric reactions.   Upon close examination of structure **6**, it was clear that achieving high enantio-selectivity in the transformation of **6** to **7** would be quite challenging

since all the stereocenters and potential coordinating groups in molecule 6 were remote from the reaction site.   Therefore, it was difficult for a chiral reagent to effectively distinguish between the two diastereotopic faces of the alkene.

For comparison, both asymmetric hydrogenation and hydroboration reaction conditions were studied. Representative reactions with selected chiral reagents are summarized in Table 1. As expected, the control reaction of **6** with hydrogen and palladium hydroxide on carbon gave no appreciable level of diastereo-selectivity, (Entry 1, *R* : *S* = 1:1). Subsequently, we surveyed a large number of chiral catalysts for their use in the asymmetric hydrogenation reaction (data not shown). Most of these reactions proved to be non-selective and the best ratio in selectivity was 2:1 favoring the *R* isomer (Entry 2). Catecholborane and *S*-alpine boramine-promoted hydroboration reactions did not provide the desired product. However, the reaction of **6** with *S*-isopinocampheyl borane (*S*-Ipc-BH$_2$) in CH$_2$Cl$_2$ at 0 °C went smoothly and exhibited a low level of diastereo-selectivity in favor of the *R* isomer (Entry 5, ratio 3:1). It is worth noting that *S*-Ipc-BH$_2$ was generated freshly from *S*-alpine boramine and BF$_3$•OEt$_2$ in THF at rt for 1.5 h. After significant optimization, the hydroboration reaction conditions that gave the most favorable results were determined to be *S*-Ipc-BH$_2$ in CH$_2$Cl$_2$ at -30 °C for 6 h, affording **7** with a very good level of enantio-selectivity in favor of the *R* isomer after hydrogenolysis (Entry 6, ratio 8:1). It is important to note that the same reaction did not produce any desired product when THF was used as the solvent in place of CH$_2$Cl$_2$ (Entry 7).

Using the optimal reaction conditions (*S*-Ipc-BH$_2$ in CH$_2$Cl$_2$ at -30 °C for 6 h), the hydroboration-oxidation reaction of **6** gave the intermediate alcohol **6a** in 87% yield after a column purification. The stereochemistry of the alcohol resulting from the hydroboration-oxidation sequence was not determined, since it was inconsequential for the next step. Hydrogenolysis of **6a** followed by a chiral supercritical fluid chromatography (SFC) provided **7a** as a single isomer in 77% yield and with >99% purity. Saponification of **7a** gave the homochiral analog **4a** in 95% yield with isomeric purity >99.8%. In 12 steps, the overall synthetic yield of **4a** from **5** is ~21%, a significant improvement compared to the original synthesis (<1%, 11 steps). Using the improved synthetic route, we prepared more than 15 grams of **4a** which was used for

supporting various in vivo studies (vide infra). Previously, we determined the absolute stereochemistry of **4a** by single crystal X-ray structure.[17] The NMR and chiral HPLC analytical data of **4a** matched perfectly with the original analytical data. Saponification of diastereoisomer **7b** provided the minor isomer **4b**. To complete the structure–activity relationship (SAR) study, we were interested in profiling both diastereoisomers **4a** and **4b**.
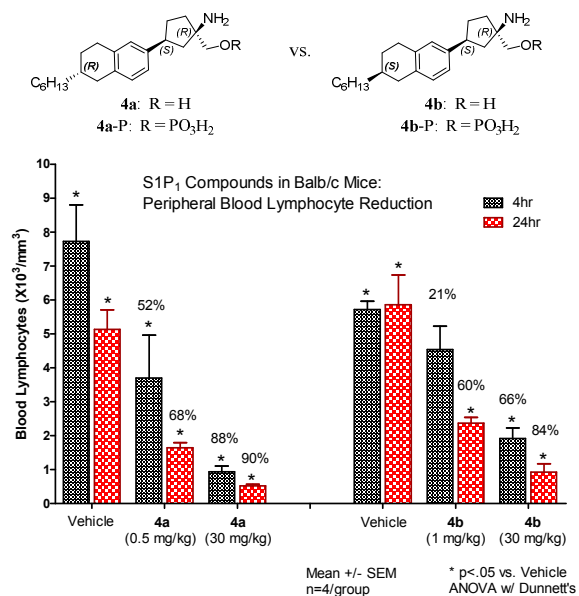
Figure 3. Lymphocyte reduction in mouse comparing **4a** and diastereoisomer **4b**.

Table 2. In Vitro Characterization of **4a**-P vs **4b**-P

Assay	**4a**-P	**4b**-P
hS1P$_1$ HLE GTPγS Binding (EC$_{50}$, nM), Y_{max} (agonist)	6.4 ± 7.6 (n = 11), 72%	60 ± 9 (n = 6), 47%
hS1P$_3$ GTPγS (EC$_{50}$, nM) (agonist)	>1000 (n = 7)	>1000 (n = 6)

| hS1P$_3$ GTPγS (IC$_{50}$, nM), (antagonist) | >1000 (n = 3) | >1000 (n = 4) |

RESULTS AND DISCUSSION

As discussed above, lymphopenia induced by the functional antagonism at S1P$_1$ is a key aspect of the clinical efficacy of **4c**.[21,22] We therefore studied the effects of **4a** and **4b** on the reduction of circulating lymphocytes in the mouse Blood Lymphocyte Reduction assay (BLR) (Figure 3). Mice (four per group) were dosed orally with the compounds dissolved in polyethylene glycol and peripheral blood lymphocyte counts were assessed at 4 and 24 hours later, respectively. A trend of greater lymphocyte reduction at 24-hour than that measured at the 4-hour time point was evident for both **4a** and **4b** at each dose level (Figure 3). This was consistent with the observation that the appearance of the active metabolite (**4a**-P or **4b**-P) for these compounds was delayed, with greater phosphate concentration in blood at 24-hour as compared to 4-hour.[23] Treatment with **4a** (0.5 or 30 mg/kg) resulted in a dose dependent reduction of peripheral blood lymphocytes of 68–90% at the 24-hour time point. It is worth noting that **4a** revealed higher levels of lymphocyte reduction at *0.5 mg/kg* than that of **4b** at *1 mg/kg* with respect to their own vehicle (e.g., lymphopenia at 24 h: **4a**-68% vs. **4b**-60%). A similar trend was also recorded for the groups dosed at 30 mg/kg (e.g., lymphopenia at 24 h: **4a**-90% vs. **4b**-84%). The data derived from the BLR assay as shown in Figure 3 indicated that **4a**, with an EC$_{50}$ of 7.9 nM for the corresponding active phosphate **4a**-P, was more potent than its isomer **4b** (phosphate **4b**-P EC$_{50}$ of 35 nM). The fact that **4a** was more efficacious than **4b** in the BLR assay indicates the importance of stereochemistry of the *n*-hexyl side chain on the reduction of blood lymphocytes. The observed in vivo results are also in agreement with our in vitro findings (Table 2). Phosphates **4a**-P and **4b**-P,[24] the active metabolites of **4a** and **4b**, respectively, were characterized in the GTPγS assay for both hS1P$_1$ and hS1P$_3$. Against hS1P$_1$ both **4a**-P and **4b**-P were found to be partial agonists (Y_{max} 74% and 47% respectively) with **4a**-P being more potent (Table 2). Both **4a**-P and **4b**-P were inactive in the hS1P$_3$ GTPγS assay in either agonist or antagonist mode. Compound **4a** was profiled in vitro in liability assays and advanced for in vivo evaluation in rodent models of chronic inflammation.
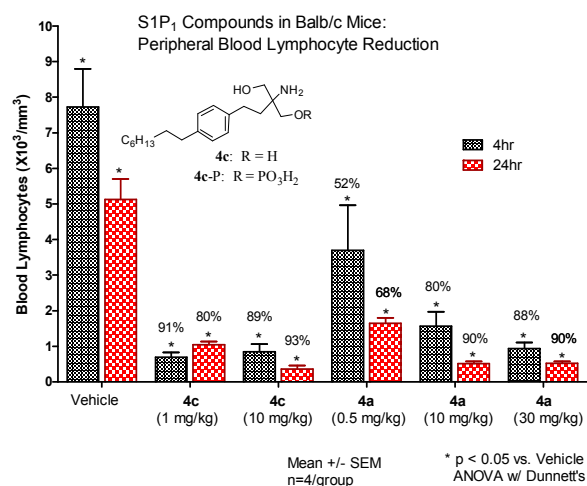
Figure 4. Lymphocyte reduction in mouse comparing **4a** and **4c**.

Table 3. General Profiles of **4c** and **4a**

Assay	4c	4a
hS1P$_1$ GTPγS (EC$_{50}$, nM)	796 ± 233 (n = 3)	2065 ± 67 (n = 3)
hERG patch clamp: % Inh @ 0.3 μM	28	36
Na$^+$ flux IC$_{50}$, μM	> 80	> 80
CYP IC$_{50}$, μM: 3A4 / 2D6 2C8 / 2C9 / 2C19	10.4 / 13.3 3.2 / 10.7 / 25	19 / > 20 5.0 / >20 / >20
LM $T_{1/2}$, min: human / rat mouse / monkey	120 / 120 120 / 35	107 / 120 120 / 120
Protein binding (h/r/m/c/d)	all < 1% free	all < 1% free

Figure 4 illustrates the comparative effects of **4a** and **4c** on the reduction of circulating lymphocytes in the mouse BLR assay. A single oral dose of **4c** (1 or 10 mg/kg) significantly reduced peripheral lymphocyte counts by 80–93% at 24 hours. Notably, the maximal degree of lymphopenia was comparable between **4a** and **4c**, as was the EC$_{50}$ of the corresponding phosphates (7.9 nM for **4a**-P vs. 5.6 nM for **4c**-P). Compound **4a** was profiled for S1P$_1$ activity, CYP inhibition, channel selectivity, and half-life ($T_{1/2}$) determination in liver microsomes (Table 3). As expected, the parent compound **4a** carried little activity

against S1P$_1$ receptor in the GTPγS assay (IC$_{50}$ = 2065 nM). With regard to ion channel selectivity, **4a** showed 36% inhibition at 0.3 μM in a hERG patch clamp assay and IC$_{50}$ > 80 μM in a Na$^+$ channel flux assay. The CYP450 inhibition IC$_{50}$ profile of **4a** was in the micromolar range. At clinically relevant concentrations, drug interactions involving the inhibition of the major drug-metabolizing CYPs are not anticipated with **4a**. The half-lives of **4a** upon incubation with human, rat, and mouse liver microsomes were long ($T_{1/2}$ >100 min) and **4a** was also found to be highly protein bound in all tested species (<1% free in human, rat, mouse, cyno and dog). In general, we found the in vitro profiles of **4a** and **4c** to be similar (Table 3).
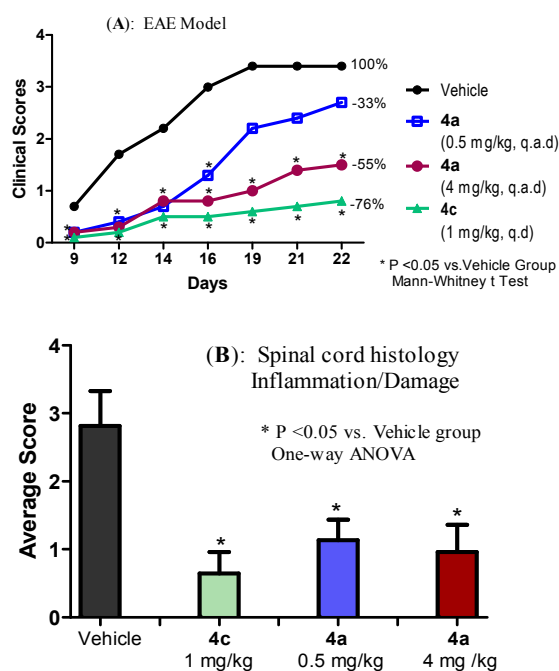
Figure 5. **4a** in MOG peptide induced mouse EAE model, clinical score (A) and histological evaluation (B). *Dosing Regimen: 4a (every other day), 4c (daily).*

The in vivo efficacy of **4a** was evaluated in a chronic model of MOG peptide induced mouse EAE (Figure 5). For comparison, **4c** was also included in this study and dosed at 1 mg/kg (*daily*, po). The mouse in vivo $T_{1/2}$ of **4a** was longer than that of **4c** (**4a**: 98 h vs. **4c**: 25 h). With the long $T_{1/2}$ of **4a**, it was dosed every other day (q.a.d.) to avoid excessive accumulation, while **4c** was dosed once daily. Oral dosing of **4a** at 0.5 and 4 mg/kg (q.a.d.) was initiated on day 1, and cumulative clinical scores were

determined. The data indicated that the level of clinical efficacy obtained was proportional to the dose of

4a administered, and there was a significant improvement in clinical scores of the mice in the highest

dosage group, with the lower dose giving intermediate effects (Figure 5, **A**). The pattern of clinical

response for **4a** at 4 mpk q.a.d. was similar to that of **4c** at 1 mpk q.d. and revealed 55% reduction in

clinical score at day 22 relative to the vehicle (vs. 76% for **4c**, Figure 5, **A**).

Histological evaluation of lumbar spinal cords were performed on day 22 to investigate the effect of **4a**

on the formation of inflammatory lesions in the CNS. Inflammatory lesions were readily detectable in

control mice, whereas the spinal cords from mice administered **4a** exhibited a marked reduction in central

nervous system damage (Figure 5, **B**). When comparing all groups using one way ANOVA and Tukey's

post test, **4c** and **4a** were significantly different from the control group in the categories of tissue damage

and inflammation ($p < 0.05$). Therefore, inhibition of EAE development by **4a** could be a result of

inhibiting encephalitogenic T cell responses and/or their migration into the CNS. These findings have

identified **4a** as a possible therapeutic agent for the treatment of multiple sclerosis.
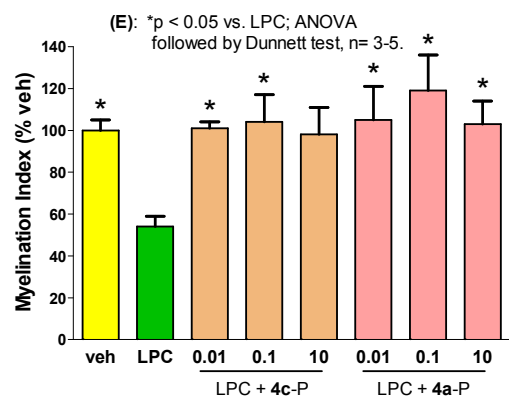

(A): Vehicle   **(B)**: LPC only
(C): LPC + 0.1 nM **4c**-P   **(D)**: LPC + 0.1 nM **4a**-P

Green: axon; Red: myelin;
Yellow: myelinated axon (axon + myelin).
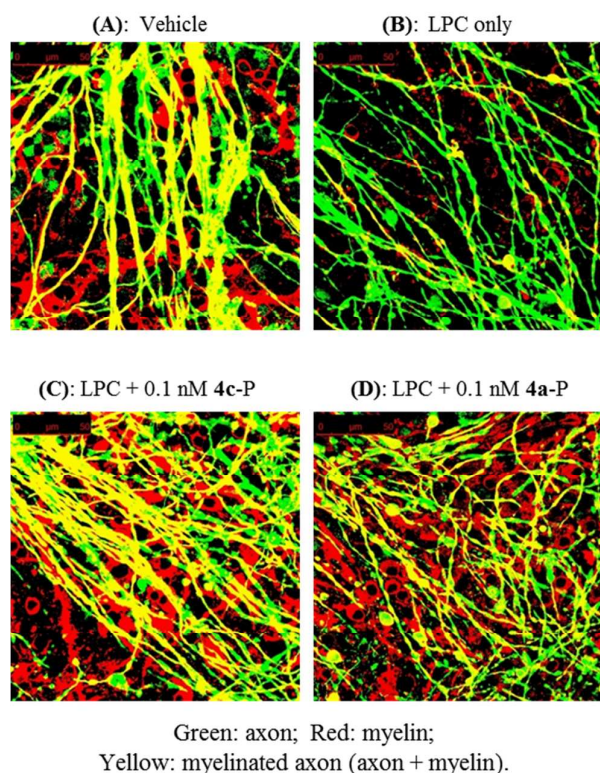
Figure 6. Effects of **4c**-P and **4a**-P on LPC-induced demyelination in organotypic cerebellar slices.

To understand the mechanism involved in suppressing EAE by administering **4a**, we evaluated **4a**-P, the active phosphorylated form of **4a**, in a three-dimensional brain cell culture assay to test if it attenuated demyelination (Figure 6).[25,26]   During the development of MS, myelin is attacked and destroyed by an autoimmune response, resulting in demyelination and subsequent axonal degeneration.[27]   Unlike EAE, which aims to approximate the pathophysiology of MS, the organotypic cerebellar slice culture system was used to study the remyelinating effects of **4a**-P on lysophosphatidylcholine (LPC)-induced demyelination without the complex systemic immune system interactions observed in intact animals.   Organotypic cerebellar slices retain the astrocyte and microglia elements that allow us to identify their contribution to myelination-associated processes.   Therefore, the interpretation and analysis of a remyelinating effect should be more straightforward than with EAE.

Figure 6 illustrates the effects of **4c**-P and **4a**-P on LPC-induced demyelination in the organotypic cerebellar slice. Most of the myelin sheaths around axonal fibers lost their integrity in the slice treated with LPC in comparison to that treated with vehicle (Figure 6, **A** vs. **B**). To validate the organotypic cerebellar slice culture system, we included **4c**-P as a positive control since **4c**-P is known to exhibit remyelination activity in this model.[11,28] In a recent study, both astrocytes and microglia were shown to be important for remyelination.[11]   In the same report, **4c** was found to increase the number of astrocytes and microglia, enhancing remyelination primarily through $S1P_1/S1P_5$ signaling pathways. In our remyelination studies, the organotypic cerebellar slices were incubated with 0.5 mg/mL LPC overnight and then transferred to the

culture medium for 24 h. Slices were then treated with **4c**-P or **4a**-P for 7 days before being processed for immunohistochemistry. As shown in Figure 6, **C** and **D**, most myelinated axons remained myelinated, and were not affected by LPC-induced demyelination with treatment of **4c**-P or **4a**-P. Myelination index values were then used to quantify the remyelination effects of **4c**-P and **4a**-P (Figure 6, **E**). The myelination index value of LPC-treated slices was ~50% using analysis of variance (ANOVA) followed by Dunnett test (P < 0.05). Compound **4a**-P promoted Purkinje cell axonal remyelination at 0.01–10 nM concentration range and myelination index values of **4c**-P and **4a**-P were both ~100% (Figure 6, **E**).

CONCLUSIONS

Efforts aimed at improving the synthesis of **4a** led to the discovery of the asymmetric hydroboration-oxidation reaction of **6** (Table 1). The observed high levels of diastereo-selectivity of this reaction are remarkable (Table 1, entry 6), given what has been known in the literature that *alkenes lacking coordinating groups have long been notoriously difficult to hydrogenate or hydroborate with high stereo-selelctivity.*[29,30] The current methodology provides an efficient approach to prepare this class of compounds. Expanding upon our previous work,[17] which supported the potential development of **4a** in the area of inflammatory bowel disease, the data outlined in this paper supports the development of **4a** in multiple sclerosis. Here, we have evaluated the impact of **4a** in the MOG induced mouse EAE model and found its efficacy at 4 mg/kg q.a.d. to be similar to **4c** at 1 mg/kg q.d. (Figure 5). Consistent with previous studies in colitis models, although a partial agonist of $S1P_1$ in several in vitro assays, **4a** was able to achieve efficacy similar to **4c** in the EAE model. To understand the mechanism involved in suppressing EAE by administering **4a**, we evaluated **4a**-P in the organotypic cerebellar slice culture system and showed remarkable remyelinating effects on LPC-induced demyelination (Figure 6). Reductions in EAE clinical scores were paralleled by reductions in demyelination, axonal loss, and astrogliosis. Taken together, these

findings demonstrate that administration of **4a** effectively prevents the development of disease in the mouse EAE model and therefore could find utility in the treatment of human MS.

EXPERIMENTAL SECTION

Chemistry. All commercially available chemicals and solvents were used without further purification. Reactions are performed under an atmosphere of nitrogen. All new compounds gave satisfactory ^{1}H NMR, LC/MS and/or HRMS, and mass spectrometry results. ^{1}H NMR spectra were obtained on a Bruker 400 MHz or a Jeol 500 MHz NMR spectrometer using residual signal of deuterated NMR solvent as internal reference. Electrospray ionization (ESI) mass spectra were obtained on a Water Micromass ESI-MS single quadrupole mass spectrometer. The purity of tested compounds determined by analytical HPLC was >95%. Analytical HPLC conditions **A**: analytical HPLC was performed on a Shimadzu instrument: column, 1-Waters Sunfire C18 2.1 x 30 mm; gradient elution 0–100% B over 4 min with 1 min hold (solvent A, 90% water/10% MeOH/0.1% TFA; solvent B, 90% MeOH/10% water/0.1% TFA; flow rate, 1 mL/min; 220 nm as the detection wavelength. Analytical HPLC conditions **B**: analytical HPLC was performed on a Shimadzu instrument: column, YMC Combiscreen ODS-A, 4.6 mm × 50 mm; gradient elution 0–100% B over 4 min with 1 min hold (solvent A, 90% water/10% MeOH/0.2% H_3PO_4; solvent B, 90% MeOH/10% water/0.2% H_3PO_4; flow rate, 4 mL/min; 220 nm as the detection wavelength.

((1R,3S)-1-Amino-3-((R)-6-hexyl-5,6,7,8-tetrahydronaphthalen-2-yl)cyclopentyl)methanol (4a, Scheme 2). To a solution of **7a** (2.35 g, 6.61 mmol) in dioxane (40 mL) was added water (10 mL) and lithium hydroxide hydrate (2.77 g, 66.1 mmol). The reaction mixture was stirred at 100 °C for 20 h. LC-MS indicated that the reaction was done and the mixture was cooled to 50 °C and filtered. The solid was washed with 1,4-dioxane (3 x 5 mL) and filtered each time, the combined filtrates were added water (45 mL) dropwise with stirring. The solid was collected with filtration and washed with water (3 x 5 mL), dried with high vacuum to give **4a** as a white solid (2.10 g 6.31 mmol, 95% yield). ^{1}H NMR (400 MHz, METHANOL-d$_4$) δ ppm: 7.06 - 6.90 (m, 3H), 3.54 - 3.40 (m, 2H), 3.01 (dd, J = 11.2, 7.1, 4.0 Hz, 1H), 2.87

- 2.71 (m, 3H), 2.35 (dd, *J* = 16.3, 10.3 Hz, 1H), 2.21 (dd, *J* = 13.1, 7.4 Hz, 1H), 2.09 - 1.87 (m, 3H), 1.84 - 1.63 (m, 3H), 1.60 - 1.49 (m, 1H), 1.46 - 1.29 (m, 11H), 0.98 - 0.87 (m, 3H). ESI-MS: *m/z* 330.35 ([M + H+]). HPLC: t_R = 3.66 min (analytical HPLC conditions **A**).

((1R,3S)-1-Amino-3-((S)-6-hexyl-5,6,7,8-tetrahydronaphthalen-2-yl)cyclopentyl)methanol **(4b, Scheme 2)** A procedure similar to that described in the synthesis of **4a** was used to prepare **4b** from **7b** (The minor product **7b** was obtained from the previous Chiral SFC preparative separation step used for the synthesis of **7a**). ^{1}H NMR (400 MHz, CHLOROFORM-d) δ ppm: 7.07 - 6.89 (m, 3H), 3.56 - 3.33 (m, 2H), 3.20 - 2.90 (m, 1H), 2.87 - 2.73 (m, 3H), 2.35 (dd, *J* = 16.3, 10.8 Hz, 1H), 2.26 (dd, *J* = 13.1, 8.0 Hz, 1H), 2.12 - 2.00 (m, 1H), 1.98 - 1.84 (m, 2H), 1.79 - 1.63 (m, 3H), 1.53 - 1.45 (m, 1H), 1.43 - 1.22 (m, 12H), 0.95 - 0.84 (m, 3H). ESI-MS: m/z 330.27 ([M + H+]). HPLC: t_R = 3.77 min (analytical HPLC conditions **B**).

(5R,7S)-7-(6-Hexyl-7,8-dihydronaphthalen-2-yl)-3-oxa-1-azaspiro[4.4]nonan-2-one (6, Scheme 2). To a solution of **15** (3.5g, 8.39 mmol) and NMP (8.07 ml, 84 mmol) in THF (200 mL) was added LiHMDS (8.39 ml, 8.39 mmol) at - 40 °C and stirred at the same temperature for 25 min followed by Ferric acetylacetonate (0.296 g, 0.839 mmol) and hexylmagnesium bromide (8.39 mL, 16.77 mmol) dropwise. The reaction mixture was stirred at - 40 to - 20 °C for 45 min then warmed to 0 °C and stirred for 15 min. The reaction mixture was diluted with water (150 mL), extracted with EtOAc (300 mL), and then washed with sat. NaHCO₃ (3 x 100 mL). The organic layer was collected, left on the bench for overnight at rt. The white solid was filtered off, and the mother liquor was dried over Na_2SO_4, concentrated on the rotavapor to give a crude product **6** which was used for the next reaction without further purification (crude yield 94%). ^{1}H NMR (400 MHz, CHLOROFORM-d), δ ppm: 7.04 - 6.91 (m, 3H), 6.21 (s, 1H), 5.06 (br s, 1H), 4.42 - 4.25 (m, 2H), 3.15 - 2.98 (m, 1H), 2.80 (t, *J* = 8.0 Hz, 2H), 2.42 - 2.09 (m, 7H), 2.05 - 1.93 (m, 2H), 1.90 - 1.78 (m, 1H), 1.54 - 1.45 (m, 2H), 1.39 - 1.29 (m, 6H), 0.99 - 0.85 (m, 3H). ESI-MS: *m/z* 354.30 ([M + H+]). HPLC: t_R = 4.23 min (analytical HPLC conditions **A**).

(5R,7S)-7-((6R)-6-Hexyl-5-hydroxy-5,6,7,8-tetrahydronaphthalen-2-yl)-3-oxa-1-azaspiro[4.4]nonan-2-one (6a, Scheme 2). To a solution of **6** (2.1 g, 5.94 mmol) in CH_2Cl_2 (10 mL) was

added dropwise to a mixture of ((1R,2S,3R,5R)-2,6,6-trimethylbicyclo[3.1.1]heptan-3-yl)borane (*S*-Ipc-BH$_2$, 0.892 g, 5.94 mmol) in 30 mL of CH$_2$Cl$_2$ (under N$_2$) at -35 °C. The mixture was stirred at -35 °C for 4 h and then at -20 °C for 2 h. MeOH (3.61 mL, 89 mmol) was added dropwise, the mixture was then stirred at -10 °C for 10 min and at 0 °C for 10 min. At 0 °C, 25 mL of THF was added then NaOH (9.90 mL, 59.4 mmol) was added dropwise followed by H$_2$O$_2$ (6.07 mL, 59.4 mmol), the mixture was stirred at rt for 16 h. The mixture was diluted with CH$_2$Cl$_2$ (100 mL) and water (50 mL), filtered through a pad of celite and the cake was washed with CH$_2$Cl$_2$ (3 x 100 mL), and the filtrate was separated and the aqueous layer was extracted with CH$_2$Cl$_2$ (50 mL). The combined CH$_2$Cl$_2$ was washed with water (100 mL) and brine (100 mL), dried over Na$_2$SO$_4$ and concentrated under vacuo. The residue was purified with a 40 g isco column: EtOAc/Hexane = 0 - 50%, gradient time = 55 min, the product came out at 45% EtOAc. The isolated fractions were concentrated and dried in vacuo to give **6a** as a solid (1.9 g, 5.11 mmol, 87% yield). ^{1}H NMR (400 MHz, METHANOL-d$_4$) 7.38 (d, *J* = 8.1 Hz, 1H), 7.10 (dd, *J* = 7.9, 1.5 Hz, 1H), 6.99 (s, 1H), 4.44 - 4.25 (m, 3H), 3.11 - 2.98 (m, 1H), 2.76 (t, *J* = 6.4 Hz, 2H), 2.30 (dd, *J* = 12.9, 7.2 Hz, 1H), 2.20 - 2.04 (m, 3H), 2.01 - 1.63 (m, 5H), 1.57 - 1.46 (m, 2H), 1.35 (d, *J* = 3.5 Hz, 7H), 1.27 - 1.18 (m, 1H), 0.96 - 0.88 (m, 3H).   Instead of **6a**, the related dehydroxylation product (5R,7S)-7-(6-hexyl-7,8-dihydronaphthalen-2-yl)-3-oxa-1-azaspiro[4.4]nonan-2-one was observed in ESI-MS: *m/z* 354.23 ([M + H$^+$]). HPLC: t_R = 3.75 min (analytical HPLC conditions **A**).

(5R,7S)-7-((R)-6-Hexyl-5,6,7,8-tetrahydronaphthalen-2-yl)-3-oxa-1-azaspiro[4.4]nonan-2-one

(7a, Scheme 2). To a solution of **6a** (3.2 g, 8.61 mmol) in MeOH (30 mL) was added Pd-C (1.1 g, 1.034 mmol), the mixture was placed under vacuum and back filled with H$_2$ with a H$_2$ balloon. The reaction mixture was stirred at rt for 6 h. A solid was precipitated out. To the mixture was added EtOAc (20 mL) and the reaction was hydrogenated for 16 h. The reaction mixture was filtered through a pad of celite and the cake was washed with EtOAc, CH$_2$Cl$_2$/MeOH and EtOAc. The combined organic solvents were concentrated under vacuo and purified by preparative chiral SFC*:* Preparative Column: Chiralpak AS-H (3×25 cm, 5μm); Flow rate: 165 mL/min; 35 °C and 100 bars; Mobile Phase: CO$_2$/MeOH (65/35)*;* Detector Wavelength: 210 nm; Separation Program: Stack injection; Injection: 0.9 mL with cycle time 165

sec; Sample preparation: 0.71 g / 30 mL MeOH : DCM (9 : 1), ~24 mg/mL. The chiral separation

provided **7a** (2.35 g, 6.61 mmol, 77% yield). ^{1}H NMR (400 MHz, METHANOL-d4) δ ppm: 7.02 - 6.91

(m, 3H), 4.43 - 4.24 (m, 2H), 3.02 (tt, J = 11.0, 7.2 Hz, 1H), 2.88 - 2.72 (m, 3H), 2.41 - 2.23 (m, 2H), 2.17

- 2.04 (m, 2H), 2.01 - 1.62 (m, 5H), 1.49 - 1.30 (m, 11H), 0.98 - 0.88 (m, 3H). ESI-MS: m/z 356.30 ([M +

H^{+}]). HPLC: t_R = 4.33 min (analytical HPLC conditions **A**).

((1R,3S)-1-Amino-3-(4-bromophenyl)cyclopentyl)methanol (8, Scheme 1). K$_2$CO$_3$ (3 g, 21.71

mmol) was dissolved in water (30 mL). **5** (4.4 g, 13.15 mmol, see reference 19 for its synthesis) and ethyl

acetate (40 mL) were then added. The mixture was stirred at rt for 20 min. The aqueous layer was

separated and extracted with ethyl acetate (4 x 20 mL). The combined ethyl acetate solutions were dried

over Na$_2$SO$_4$ and concentrated under reduced pressure to give **5a** as a free base of **5**. The liquid **5a** was

dissolved in ethanol (40 mL), NaBH$_4$ (1.244 g, 32.9 mmol) was added at 0 °C portionwise. The mixture

was stirred at rt for 18 h. The reaction mixture was cooled to 0 °C and 6 N aqueous HCl was added

dropwise to quench the reaction. The suspension was stirred at rt for 30 min before 30% aqueous NaOH

was added at 0 °C. The mixture was stirred at rt for 1 h and then concentrated to remove organic solvents.

Ethyl acetate (50 mL) was added. Water (30 mL) was added to dissolve the solid and the aqueous layer was

separated and extracted with ethyl acetate (3 x 20 mL). The combined ethyl acetate solutions were dried

over K$_2$CO$_3$ and Na$_2$SO$_4$ and concentrated under reduced pressure to give **8** (3.1 g, 11.47 mmol, 87 %

yield) as a white solid. ^{1}H NMR (400 MHz, DMSO-d6), δ ppm: 7.51-7.40 (m, 2H), 7.27 (d, J = 8.4 Hz,

2H), 3.32-3.20 (m, 2H), 3.09-2.92 (m, 1H), 2.11 (dd, J = 12.9, 8.7 Hz, 1H), 1.98-1.87 (m, 1H), 1.80 (qd, J =

11.1, 7.9 Hz, 1H), 1.69-1.58 (m, 1H), 1.48 (ddd, J = 12.4, 7.9, 2.2 Hz, 1H), 1.32 (dd, J = 12.8, 10.1 Hz,

1H). ESI-MS: m/z 270.16 ([M + H^{+}]). HPLC: t_R = 1.85 min (analytical HPLC conditions **B**).

(5R,7S)-7-(4-Bromophenyl)-3-oxa-1-azaspiro[4.4]nonan-2-one (9, Scheme 1). To a cloudy solution

of **8** (3.1 g, 11.47 mmol) in THF (50 mL) was added 1,1'-Carbonyldiimidazole (2.79 g, 17.21 mmol)

portionwise. Pyridine (1.392 mL, 17.21 mmol) was then added. The reaction was stirred at rt under

nitrogen overnight. 6 N aqueous HCl (~12 mL) was added dropwise with water bath cooling to make pH

~2. The mixture was stirred at rt for 1.5 h before ethyl acetate (50 mL) was added. The aqueous layer was

separated and extracted with ethyl acetate (2 x 25 mL). The combined organic solutions were washed with 1 N aqueous HCl (25 mL), brine (25 mL), and saturated aqueous sodium bicarbonate solution (25 mL) till pH ~8, dried over Na_2SO_4, and concentrated under reduced pressure. The residue was dissolved in ethyl acetate (~50 mL) with heating and mixed with hexanes (~50 mL). The solid was filtered, washed with ethyl acetate, and dried to give **9** (3.3 g, 11.14 mmol, 97% yield) as a white solid. ^{1}H NMR (400 MHz, CHLOROFORM-d), δ ppm: 7.45 (d, J = 8.6 Hz, 2H), 7.12 (d, J = 8.4 Hz, 2H), 6.42 (br. s., 1H), 4.41-4.21 (m, 2H), 3.17-2.91 (m, 1H), 2.34 (dd, J = 13.3, 7.4 Hz, 1H), 2.23-2.11 (m, 2H), 2.01-1.90 (m, 2H), 1.88-1.74 (m, 1H). ESI-MS: m/z 296.14 ([M + H^{+}]). HPLC: t_R = 2.78 min (analytical HPLC conditions **B**).

(2-(*tert*-Butoxy)-2-oxoethyl)zinc(II) bromide (11b, Scheme 1). To a mixture of Zn (1.760 g, 26.9 mmol) dust and THF (15 mL), TMS-Cl (0.082 mL, 0.641 mmol) was added and the mixture was stirred at rt for 1 h. tert-Butyl 2-bromoacetate (5 g, 25.6 mmol) was then added dropwise to bring the temp to 50 °C and maintained at the temperature during the addition (25 min). The reaction mixture was stirred at 50 °C for 1 h. The reaction mixture was then allowed to cooled down to 10 °C and kept there for 1 h. The solid was collected with filtration and washed with THF (3 x 2 mL), dried under vacuo to give **11b** (5.4 g, 16.24 mmol, 63% yield) as a white solid. ^{1}H NMR (400 MHz, METHANOL-d4) δ ppm: 3.75 (t, J = 6.3 Hz, 4H), 1.97 - 1.93 (m, 2H), 1.92 - 1.87 (m, 4H), 1.46 (s, 9H). The ^{1}H NMR was taken as a complex of **11b** associated with one equivalent of THF (THF coordinated to the Zn in the molecule **11b**).

tert-**Butyl 2-(4-((5R,7S)-2-oxo-3-oxa-1-azaspiro[4.4]nonan-7-yl)phenyl)acetate (12, Scheme 1).** To a pressure flask (350 mL) containing **9** (5 g, 16.88 mmol) anhydrous THF (100 mL) was charged with N_2, then LiHMDS (18.57 mL, 18.57 mmol) was added with stirring. After stirred for 30 min, 1,2,3,4,5-pentaphenyl-1'-(di-t-butylphosphino)ferrocene (0.360 g, 0.506 mmol), Pd2(dba)3 (0.464 g, 0.506 mmol) and **11b** (16.84 g, 50.6 mmol) were added respectively. The mixture was flashed with N_2 for 5 min, sealed and stirred at 80 °C for 16 h. After cooling, the reaction mixture was filtered through a pad of celite and the cake was washed with EtOAc (200 mL), then water (50 mL) and 1 N HCl (100 mL) were added. The organic layer was collected and washed with 1 N HCl (2 x 100 mL), brine (2 x100 mL), dried over Na_2SO_4 and concentrated under vacuo to give the crude product **12** which was used for the next reaction as is (5.6 g,

16.90 mmol, 100% yield) as a white solid. ^{1}H NMR (400 MHz, CHLOROFORM-d), δ ppm: 7.26 - 7.16 (m, 4H), 5.59 - 5.52 (m, 1H), 4.38 - 4.27 (m, 2H), 3.53 (s, 2H), 3.14 - 3.03 (m, 1H), 2.41 - 2.31 (m, 1H), 2.15 (s, 2H), 1.97 (d, J = 1.5 Hz, 2H), 1.89 - 1.79 (m, 1H), 1.49 - 1.45 (m, 9H). ESI-MS: m/z 332.18 ([M + H$^+$]). HPLC: t_R = 3.09 min (analytical HPLC conditions **A**).

2-(4-((5R,7S)-2-Oxo-3-oxa-1-azaspiro[4.4]nonan-7-yl)phenyl)acetic acid (13, Scheme 1). To a mixture of **12** (5.6 g, 16.90 mmol) in CH$_2$Cl$_2$ (50 mL) was added TFA (25 mL). The reaction mixture was stirred at rt for 1.5 h. The solvent was removed under vacuo and the residue was dissolved in EtOAc (150 mL) and 1 N NaOH (100 mL). The organic layer was separated, collected, and extracted with 1 N NaOH (100 mL). The aqueous layers were combined and acidified with conc. HCl to pH = 1-2 and then was extracted with EtOAc (2 x 100 mL), which was washed with brine (100 mL), dried over Na$_2$SO$_4$ and concentrated under vacuo to give **13** (4.45 g, 16.16 mmol, 96% yield) as a white solid. ^{1}H NMR (400 MHz, CHLOROFORM-d), δ ppm: 7.31 (s, 1H), 7.25 - 7.17 (m, 3H), 4.38 - 4.29 (m, 2H), 3.69 - 3.65 (m, 2H), 3.16 - 3.04 (m, 1H), 2.36 (dd, J = 13.8, 8.5 Hz, 1H), 2.21 - 2.12 (m, 2H), 1.99 (dd, J = 13.8, 10.2 Hz, 1H), 1.93 - 1.79 (m, 2H). ESI-MS: m/z 276.12 ([M + H$^+$]). HPLC: t_R = 2.13 min (analytical HPLC conditions **A**).

(5R,7S)-7-(6-Oxo-5,6,7,8-tetrahydronaphthalen-2-yl)-3-oxa-1-azaspiro[4.4]nonan-2-one (14, Scheme 1). To a mixture of **13** (0.5 g, 1.816 mmol) in CH$_2$Cl$_2$ (13 mL) was added oxalyl chloride (0.477 mL, 5.45 mmol) followed by a few drops of DMF. After 1 h, an aliquot was quenched in MeOH and checked by LCMS for the methyl ester. LCMS showed a complete conversion to the acid chloride. Reaction mixture was concentrated in vacuo and dried. Residue was re-dissolved in CH$_2$Cl$_2$ (13 mL) in a glass pressure vessel. Ethylene was bubbled through for 3 min at -78 °C before aluminum chloride (0.727 g, 5.45 mmol) was added. Ethylene was bubbled through for 7 more min then the reaction was sealed and allowed the reaction to slowly warm to rt over 1 h. Sonication broke down the chunk. The mixture was stirred at rt for 1.5 h. The reaction mixture was poured on to ice. The reaction mixture was diluted with dichloromethane. The aqueous layer was extracted with CH$_2$Cl$_2$. The combined organic layers were washed with 1M HCl, dried over Na$_2$SO$_4$, filtered and conc. The crude material was purifed on a silica gel

cartridge (12 g) using an ethyl acetate / hexanes gradient (20-100%) to give **14** (0.33 g, 1.157 mmol, 64%

yield) as a yellow solid. ^{1}H NMR (400 MHz, CHLOROFORM-d), δ ppm: 7.20-7.00 (m, 3H), 5.49 (br. s.,

1H), 4.45-4.25 (m, 2H), 3.59 (s, 2H), 3.08 (t, J = 6.8 Hz, 3H), 2.58 (t, J = 6.7 Hz, 2H), 2.38 (dd, J = 13.2,

7.3 Hz, 1H), 2.27-2.11 (m, 2H), 2.05-1.92 (m, 2H), 1.92-1.74 (m, 1H). ESI-MS: m/z 286.14 ([M + H$^+$]).

HPLC: t_R = 2.18 min (analytical HPLC conditions **B**).

6-((5R,7S)-2-Oxo-3-oxa-1-azaspiro[4.4]nonan-7-yl)-3,4-dihydronaphthalen-2-yl

trifluoromethanesulfonate (15, Scheme 2). To a mixture of **14** (1.8 g, 6.31 mmol) and DMPU (2.282 mL,

18.92 mmol) in THF (50 mL) was added LDA (9.46 mL, 18.92 mmol) dropwise. The reaction mixture was

stirred for 30 min then 1,1,1-trifluoro-N-phenyl-N-(trifluoromethyl)sulfonyl methanesulfonamide (4.51 g,

12.62 mmol) in THF (10 mL) was added. The reaction mixture was warmed to 0 °C and stirred for 1 h.

LCMS showed conversion to be complete. The reaction mixture was diluted with water (5 mL), ethyl

acetate (40 mL) and washed with sat NaCl (20 mL). The organic layer was collected, dried over MgSO$_4$,

and concentrated. The crude material was purified on a silica gel cartridge (80 g) using an EtOAc/Hex

gradient (0-100% EtOAc over 20 minutes). Isolated product-containing fractions, concentrated and dried

in vacuo to give **15** as an oil (1.8 g, 4.31 mmol, 68.4 % yield). ^{1}H NMR (400 MHz, CHLOROFORM-d)

δ 7.05 (s, 2H), 7.02 (s, 1H), 6.49 (s, 1H), 5.66 (s, 1H), 4.42 - 4.23 (m, 2H), 3.07 (t, J = 8.4 Hz, 2H), 2.80 -

2.64 (m, 2H), 2.35 (dd, J = 13.4, 7.3 Hz, 1H), 2.23 - 2.09 (m, 2H), 2.05 - 1.88 (m, 3H), 1.89 - 1.77 (m, 1H).

ESI-MS: m/z 418.06 ([M + H$^+$]). HPLC: t_R = 3.57 min (analytical HPLC conditions **A**).

Biological Assays. *Receptor HLE [^{35}S] GTPγS Binding Assays.* Compounds were loaded in a 384

Falcon V-bottom plate (0.5 μL/well in a 3-fold dilution). Membranes prepared from S1P1/CHO cells or

EDG3-Ga15-bla HEK293T cells were added to the compound plate (40 μL/well, final protein 3 μg/well)

with multidrop. [^{35}S]GTP (1250 Ci/mmol, PerkinElmer) was diluted in assay buffer: 20 mM HEPES, pH

7.5, 10 mM MgCl$_2$, 150 mM NaCl, 1 mM EGTA, 1 mM DTT, 10 μM GDP, 0.1% fatty acid free BSA, and

10 μg/mL saponin to 0.4 nM. Then 40 μL of the [^{35}S] GTP solution was added to the compound plate with

a final concentration of 0.2 nM. The reaction was kept at room temperature for 45 min. At the end of

incubation, all the mixtures in the compound plate were transferred to a 384-well FB filter plates via GPCR

robot system. The filter plate was washed with water four times by using the modified manifold Embla

plate washer and dried at 60 °C for 45 min. Then 30 μL of MicroScint 20 scintillation fluid was added to

each well for counting at Packard TopCount. EC_{50} is defined as the agonist concentration that corresponds

to 50% of the Y_{max} (maximal response) obtained for each individual compound tested.

Blood Lymphocyte Reduction Assay (BLR) in Rodents. Balb/c mice were dosed orally with test article

(as a solution or suspension in the vehicle) or vehicle alone (polyethylene glycol 300, PEG300). Blood was

drawn at 4 h and at 24 h by retro-orbital bleeding. Blood lymphocyte counts were determined on an

ADVIA 120 hematology analyzer (Siemens Healthcare Diagnostics). The results were measured as a

reduction in the percentage of circulating lymphocytes as compared to the vehicle treated group at the 4 and

24 h measurements. The results represent the average results of all animals within each treatment group (n

= 3−4).

hERG Patch Clamp Assay. Whole-cell patch-clamp was used to directly measure hERG currents in

HEK 293 cells stably expressing the cloned hERG potassium channel α subunit. The compound was tested

in an aqueous buffer with pH 7.4 at room temperature. Repetitive test pulses (0.05 Hz) were applied from a

holding potential of 80 mV to +20 mV for 2 seconds and tail currents were elicited following the test pulses

by stepping the voltage to 65 mV. The effects from the compound were calculated by measuring inhibition

of peak tail current

Mouse Experimental Autoimmune Encephalomyelitis Assay (EAE). Mice (C57BL/6 female, 6-8 weeks

of age, Charles River, n=10 treatment group) were immunized subcutaneously with 150 mg MOG_{35-55}

emulsified 1:1 with Incomplete Freund's Adjuvant (Sigma) supplemented with 150 mg mycobacterium

tuberculosis H37RA (Difco Laboratories). Then 400 ng of pertussis toxin (CalBiochem) was injected

intraperitoneally on the day of immunization and 2 days later. Clinical scoring and body weight were taken

3 times per week. Clinical scoring system: 0.5: partial tail weakness; 1: limp tail or waddling gait with tail

tonicity; 1.5: waddling gait with partial tail weakness; 2: waddling gait with limp tail (ataxia); 2.5: ataxia

with partial limb paralysis; 3: full paralysis of one limb; 3.5: full paralysis of one limbs with partial

paralysis of a second limb; 4: full paralysis of two limbs; 4.5: moribund; 5: death. Mean clinical score was

calculated by averaging the scores of all mice in each group. Upon termination of the study, spinal

columns were excised and submersion fixed in 10% Neutral Buffered Formalin. Three transverse sections

of lumbar spinal cord were routinely processed, paraffin embedded (RPPE) and were sectioned at 3μm and

6um, stained with hematoxylin and eosin and the myelin-specific stain Luxol Fast Blue, respectively.

Slides were analyzed in a blinded fashion for severity of inflammation, tissue damage, and demyelination.

Lesion activity was scored on a semi-quantitative 0-5 scale, and overall mean histological score of

inflammation, damage, and demyelination from each group was calculated.

Organotypic Cerebellar Slice Culture Assay. Newborn (P1-2) wild-type CD1 mouse pups were

obtained from Charles River. After decapitation, the cerebellum was isolated and cut into 350 um

parasagittal slices. Slices were then transferred to culture inserts (Millipore Millicell-CM organotypic

culture inserts) in a 6-well plate with 1 ml culture medium, and incubated at 36–37∘C with 5% CO_2.

Culture medium was composed of 50% minimal essential media, 25% heat-inactivated horse serum, 25%

Earle's balanced salt solution, 6.5 mg/ml glucose (Sigma-Aldrich, St-Louis, MO), and penicillin and

glutamine supplements (All from Invitrogen, Carlsbad, CA), and was replaced every 2–3 days. Slices were

cultured for 13 days *in vitro* (DIV13) to allow clearance of debris and myelination to occur. For

remyelination studies, slices were incubated with 0.5 mg/ml LPC for overnight, and then transferred to the

culture medium for 24 h. Afterward, slices were treated with **4c**-P or **4a**-P for 7 days before being

processed for immunohistochemistry.

Cerebellar slices were fixed with 4% paraformaldehyde and incubated with rat anti-myelin basic protein

(MBP, 1:1000, Abcam) and rabbit anti-calbindin D-28K (CBD, 1: 4000, Swant, Switzerland) at 4 °C

overnight. MBP and CBD were used for visualizing myelin protein and Purkinje cell bodies and axonal

processes, respectively. The slices were incubated with 1:500 goat anti rat IgG Alexa Fluor 594 and goat

anti-rabbit IgG Alexa Fluor 488 (Life Technologies), and then mounted and cover slipped. A SP8 confocal

microscopy was used for immunofluorescence image acquisition. MBP and CBD immunostaining was imaged at

×40 magnification, and multiple images were captured from each slices. The areas covered by axonal processes

singly stained for CBD or doubly stained for CBD and MBP immunoreactivity were analyzed using a macro with

Image-J (NIH). The Myelination Index was calculated by dividing CBD+MBP double immunoreactivity/area unit with CBD single immunoreactivity/area unit as a measure of the amount of myelination per axon area. Quantitative data were analyzed statistically using ANOVA, followed by the Dunnett's Multiple Comparison Test.

AUTHOR INFORMATION

Corresponding Authors

*M.G.Y.: Phone, 609-252-3234; E-mail, michael.yang@bms.com

*A.J.D.: Phone, 609-252-3593; E-mail, alaric.dyckman@bms.com

ABBREVIATIONS USED

BLR, blood lymphocyte reduction assay; CDI, carbonyldiimidazole; CNS, central nervous system; EAE, experimental autoimmune encephalomyelositis; S-Ipc-BH$_2$, S-isopinocampheyl borane; LiHMDS, lithium bis(trimethylsilyl)amide; LDA, lithium diisopropylamide; LPC, lysophosphatidylcholine; MS, multiple sclerosis; S1P, sphingosine-1-phosphate; SFC, supercritical fluid chromatography.

REFERENCES

1. Costello, K.; Halper, J.; Kalb, R.; Skutnik, L.; Rapp, R. The Use of Disease-Modifying Therapies in Multiple Sclerosis: Principles and Current Evidence, **2016**. National Multiple Sclerosis Society. http://www.nationalmssociety.org/getmedia/5ca284d3-fc7c-4ba5-b005-ab537d495c3c/DMT_Consensus_MS_Coalition_color (accessed November 22, 2016).

2. Genain, C. P.; Cannella, B.; Hauser, S. L.; Raine, C. S. Identification of autoantibodies associated with myelin damage in multiple sclerosis. *Nat. Med.* **1999**, *5*, 170-175.

3. Serafini, B.; Rosicarelli, B.; Magliozzi, R.; Stigliano, E.; Aloisi, F. Detection of ectopic B-cell follicles with germinal centers in the meninges of patients with secondary progressive multiple sclerosis. *Brain Pathol*. **2004**, *14*, 164-174.

4. (a) Fletcher, J. M.; Lalor, S. J.; Sweeney, C. M.; Tubridy, N.; Mills, H. H. G. T cells in multiple sclerosis and experimental autoimmune encephalomyelitis. *Clin. Exp. Immunol*. **2010**, *162*, 1-11. (b) Disanto, G.; Morahan, J. M.; Barnett, M. H.; Giovannoni, G.; Ramagopalan, S. V. The evidence for a role of B cells in multiple sclerosis. *Neurology* **2012**, *78*, 823-832.

5. Lehmann-Horn, K.; Kronsbein, H. C.; Weber, M. S. Targeting B cells in the treatment of multiple sclerosis: recent advances and remaining challenges. *Ther. Adv. Neurol. Disord*. **2013**, *6*, 161-173.

6. (a) Rosen, H.; Goetz, E. J. Sphingosine 1-phosphate and its receptors: an autocrine and paracrine network. *Nat. Rev. Immunol.* **2005**, *5*, 560-570. (b) Hla, T. Physiological and pathological actions of sphingosine 1-phosphate. *Semin. Cell. Dev. Biol*. **2004**, *15*, 513-520.

7. (a) Matloubian, M.; Lo C. G.; Cinamon, G.; Lesneski, M, J.; Xu, Y.; Brinkmann, V.; Allende, M. L.; Proia, R. L; Cyster, J. G. Lymphocyte egress from thymus and peripheral lymphoid organs is dependent on S1P receptor 1. *Nature* **2004**, *427*, 355-360. (b) Mandala, S.; Hajdu, R.; Bergstorm, J.; Quackenbush, E.; Xie, J.; Milligan, J.; Thornton, R.; Shei, G-J.; Card, D.; Keohane, CA.; Rosenbach, M.; Hale, J.; Lynch, C. L.; Rupprecht, K.; Parsons, W.; Rosen, H. Alteration of lymphocyte trafficking by sphingosine-1-phosphate receptor agonists. *Science* **2002**, *296*, 346-349.

8. Hun, J.; Hartung, H. P. A. P.; Mechanism of action of oral fingolimod (FTY720) in multiple scelrosis. *Clin. Neuropharmacol.* **2010**, *33*, 91-101.

9. The EC_{50} of **4c**-P and the EC_{50} of **4a**-P were comparable as tested in the internalization assay. However, compound **4c**-P was a full agonist with a maximal response in inducing $S1P_1$ internalization (Y_{max} 100%). Unlike **4c**-P, compound **4a**-P was shown to be a partial agonist (Y_{max} 68%). For more information see reference 17.

10. (a) Subei, A. M.; Cohen, J. A. Sphingosine 1-phosphate receptor modulators in multiple sclerosis. *CNS Drugs* **2015**, *29*, 565-575. (b) Brinkmann, V.; Davis, M. D.; Heise, C. E.; Albert, R.; Cottens, S.;

Hof, R.; Bruns, C.; Prieschl, E.; Baumruker, T.; Hiestand, P.; Foster, C. A.; Zollinger, M.; Lynch, K. R. The immune modulator FTY720 targets sphingosine 1-phosphate receptors. *J. Biol. Chem.* **2002**, *277*, 21453-21457.

11. Miron, V. E.; Ludwin, S. K.; Darlington, P. J.; Jarjour, A. A.; Soliven, B.; kennedy, T. E.; Antel, J. P. Fingolimod (FTY720) enhances remyelination following demyelination of organotypic cerebellar slices. *Am. J. Pathol.* **2010**, *176*, 2682-2694.

12. (a) Yoshida, Y.; Tsuji, T.; Watanabe, S.; Matsushima, A.; Matsushima, Y.; Banno, R.; Fujita, T.; Kohno, T. Efficacy of combination treatment with fingolimod (FTY720) plus pathogenic autoantigen in a glucose-6-phosphate isomerase peptide (GPI325-339)-induced arthritis mouse model. *Biol. Pharm. Bull.* **2013**, *36*, 1739-1746. (b) Matsuura, M.; Imayoshi, T.; Okumoto, T. Effect of FTY720, a novel immunosuppressant, on adjuvant- and collagen-induced arthritis in rats. *Int. J. Immunopharmacol.* **2000**, *22*, 323-331.

13. Gonzalez-Cabrera, P. J.; Brown, S.; Studer, S. M.; Rosen, H. S1P signaling: new therapies and opportunities. *F1000Prime Rep.* **2014**, *6*, 109-116.

14. Nofer, J. R.; Bot, M.; Brodde, M.; Taylor, P. J.; Salm, P.; Brinkmann. V.; van Berkel, T.; Assmann, G.; Biessen, E. A. FTY720 a synthetic sphingosine 1 phosphate analogue, inhibits development of atherosclerosis in low-density lipoprotein receptor-deficient mice. *Circulation* **2007**, *115*, 501-508.

15. (a) Kappos, L.; Antel, J.; Comi, G.; Montalban, X.; O'Connor, P.; Polman, C. H.; Haas, T.; Korn, A. A.; Karlsson, G.; Radue, E. W. Oral fingolimod (FTY720) for relapsing multiple sclerosis. *N. Engl. J. Med.* **2006**, *355*, 1124-1140. (b) Cohen, J. A.; Barkhof, F.; Comi, G.; Hartung, H. P.; Khatri, B. O.; Montalban, X.; Pelletier, J.; Capra, R.; Gallo, P.; Izquierdo, G.; Tiel-Wilck, K.; de Vera, A.; Jin. J.; Stites, T.; Wu, S.; Aradhye, S.; Kappos, L. Oral fingolimod or intramuscular interferon for relapsing multiple sclerosis. *N. Engl. J. Med.* **2010**, *362*, 402-415.

16. Lehman-McKeeman, L. D.; Dyckman, A. J.; Taylor, T.; Yang, X.; Shen, D. R.; Thomas, R.; Borowski, V.; Tang, H.; Heimrich, E.; Xiao, H. Y.; Gilmore, J.; Sheppeck, J.; Dhar, T. G. M.; Cornelius1, G.; Marino, A.; Lecureux, L.; D'Arienzo, C.; Sun, H.; Yang, Z.; Kukral, D.; Banas, D.; Suchard. S.; Cvijic,

M. E.; Mcintyre, K. W.; Salter-Cid, L.; Xie, J. H. Unpublished results. A differentiated sphingosine-1-phosphate immune modulator with reduced risk for vascular leak. Manuscript in preparation.

17. Dhar, T. G. M. Xiao, H. Y.; Xie, J.; Lehman-McKeeman, L. D.; Wu, D. R.; Dabros, M.; Yang, X.; Taylor, T.; Zhou, X.; Heimrich, E.; Mcintyre, K. W.; Warrack, B.; Shi, H.; Levesque, P. C.; Zhu, J. L.; Hennan, J.; Balimane, P.; Yang, Z.; Marino, A. M.; Cornelius, G.; D'Arienzo, C. J.; Mathur, A.; Shen, D. R.; Cvijic, M. E.; Salter-Cid, L.; Barrish, J. C.; Carter, P. H.; Dyckman, A. J. Identification and preclinical pharmacology of BMS-986104: A differentiated S1P$_1$ receptor modulator in clinical trials. *ACS Med. Chem. Lett.* **2016**, *7*, 283-288.

18. The full in vitro and in vivo data set on **4a**-P formation associated with SphK2 will be published in the near future (reference 16, manuscript in preparation).

19. Wallace, G. A.; Gordon, T. D.; Hayes, M. E.; Konopacki, D. B.; Fix-Stenzel, S. R.; Zhang, X.; Grongsaard, P.; Cusack, K. P.; Schaffter, L. M.; Henry, R. F.; Stoffel, R. H. Scalable synthesis and isolation of the four stereoisomers of methyl 1-amino-3-(4-bromophenyl)cyclopentanecarboxylate, useful intermediates for the synthesis of S1P$_1$ receptor agonists. *J. Org. Chem.* **2009**, *74*, 4886-4889.

20. Malecha, J. W.; Fraher, T. P. Method for the preparation of a chiral-beta-amino ester. WO0051968, Nov 9, 2000.

21. Chiba, K.; Matsuyuki, H.; Maeda, Y.; Sugahara, K. Role of sphingosine 1-phosphate receptor type 1 in lymphocyte egress from secondary lymphoid tissues and thymus. *Cell. Mol. Immunol.* **2006**, *3*, 11-19.

22. Mullershausen, F.; Zecri, F.; Cetin, C.; Billich, A.; Guerini, D.; Seuwen, K.   Persistent signaling induced by FTY720-phosphate is mediated by internalized S1P$_1$ receptors. *Nat. Chem. Biol.* **2009***, 5*, 428-434.

23. The phosphate to parent *AUC$_{0-24h}$* ratios as measured in mouse plasma were 0.51 and 0.57 for **4a**-P/**4a** and **4b**-P/**4b**, respectively.

24. The synthesis of phosphates, such as **4a**-P, can be achieved from the reaction of phosphorus pentoxide and phosphoric acid followed by the addition of **4a** or **4b** with stirring at 100 °C under nitrogen for

several hours. A detailed experimental procedure can be found in the Supporting Information of reference 17.

25. Merrill, J. E. In vitro and in vivo pharmacological models to assess demyelination and remyelination. *Neuropsychopharmacology* **2009**, *34*, 55-73.

26. Sheridan, G. K.; Dev, K. K. S1P$_1$ receptor subtype inhibits demyelination and regulates chemokine release in cerebellar slice cultures. *Glia* **2012**, *60,* 382-392.

27. Miller, R. H.; Mi, S. Dissecting demyelination. *Nat. Neurosci*. **2007**, *10*, 1351–1354.

28. Slowik, A.; Schmidt, T.; Beyer, C.; Amor, S.; Clarner, T.; Kipp, M. The sphingosine 1-phosphate receptor agonist FTY720 is neuroprotective after cuprizone-induced CNS demyelination. *Brit. J. Pharmacol.* **2015**, *172*, 80-92.

29. Dhokte, U. P.; Brown, H. C. Isopinocampheylbromoborane a new promising reagent for the asymmetric hydroboration of prochiral alkenes. *Tetrahedron Lett*. **1996**, *37*, 9021-9024.

30. Thomas, S. P.; Aggarwal, V. K. Asymmetric hydroboration of 1,1-disubstituted alkenes. *Angew. Chem. Int. Ed.* **2009**, 48, 1896-1898.

Table of Contents graphic